

**$\Sigma$  resonances from  $K^-N \rightarrow \pi\Lambda$  reactions with center-of-mass energies from 1550 to 1676 MeV**Puze Gao,<sup>1</sup> Jun Shi,<sup>1</sup> and B. S. Zou<sup>1,2</sup><sup>1</sup>*Institute of High Energy Physics and Theoretical Physics Center for Science Facilities, Chinese Academy of Sciences, Beijing 100049, China*<sup>2</sup>*State Key Laboratory of Theoretical Physics, Institute of Theoretical Physics, Chinese Academy of Sciences, Beijing 100190, China*

(Received 20 June 2012; revised manuscript received 29 July 2012; published 22 August 2012)

For the study of the  $\Sigma$  resonances, we analyze the differential cross sections and  $\Lambda$  polarizations for the reactions  $K^-n \rightarrow \pi^-\Lambda$  and  $K^-p \rightarrow \pi^0\Lambda$  with an effective Lagrangian approach. Data of an early experiment and the recent Crystal Ball experiment at BNL are included in the analysis with the c.m. energy from 1550 to 1676 MeV. Our results clearly support the existence of a  $\Sigma$  resonance with  $J^P = \frac{1}{2}^+$ , mass near 1633 MeV, and width about 120 MeV, which confirms the three-star  $\Sigma(1660)\frac{1}{2}^+$  in PDG. Meanwhile, our results do not support the existence of the two-star  $\Sigma(1620)\frac{1}{2}^-$  in PDG. The analysis results for the parameters of the relevant  $\Sigma$  resonances and couplings are presented.

DOI: [10.1103/PhysRevC.86.025201](https://doi.org/10.1103/PhysRevC.86.025201)

PACS number(s): 13.75.Jz, 13.75.Gx, 14.20.Jn, 25.80.Nv

**I. INTRODUCTION**

Quenched  $qqq$  quark models and unquenched  $qqq \leftrightarrow qqqq\bar{q}$  quark models give very different predictions for the  $J^P = \frac{1}{2}^-$  SU(3) nonet partners of the  $N(1535)$  and  $\Lambda(1405)$ . While quenched quark models [1–4] predict the  $J^P = \frac{1}{2}^-$   $\Sigma$  and  $\Xi$  resonances to be around 1650 and 1760 MeV, respectively, the unquenched quark models [5–7] expect them to be around 1400 and 1550 MeV, respectively, a meson-soliton bound-state approach of the Skyrme model [8] and other meson-baryon dynamical models [9,10] predict them to be around 1450 and 1620 MeV, respectively.

Although various phenomenological models give distinguishable predictions for the lowest  $J^P = \frac{1}{2}^-$   $\Sigma$  and  $\Xi$  states, none of them are experimentally established. There is relatively more information on the  $\Sigma$  resonances in the PDG tables, coming from analyses of early  $\bar{K}N$  experiments in the 1970s [11]. Some analyses are for the c.m. energy around 1600 MeV [12–15]. However, restricted by the uncertainties from low statistics and background contributions, the  $\Sigma$  resonant structures around 1600 MeV are still not very clear, and several  $\Sigma$  resonances are listed in PDG tables with only one or two stars around this region.

There is a  $\Sigma(1620)\frac{1}{2}^-$  listed as a two-star resonance in the PDG tables [11]. This seems to support the prediction of quenched quark models. However, for the two-star  $\Sigma(1620)\frac{1}{2}^-$  resonance, only four references [16–19] are listed in PDG tables with weak evidence for its existence. Among them, Refs. [16,17] are based on multichannel analyses of the  $\bar{K}N$  reactions. Both claim evidence for a  $\Sigma(\frac{1}{2}^-)$  resonance with mass around 1620 MeV, but give totally different branching ratios for this resonance. Reference [16] claims that it couples only to  $\pi\Lambda$  and not to  $\pi\Sigma$ , while Ref. [17] claims the opposite way. Both analyses do not have  $\Sigma(1660)\frac{1}{2}^+$  in their solutions. However, Ref. [12] shows no sign of  $\Sigma(\frac{1}{2}^-)$  resonance between 1600 and 1650 MeV through analysis of the reaction  $\bar{K}N \rightarrow \Lambda\pi$  with the c.m. energy in the range of 1540–2150 MeV; instead, it suggests the existence of  $\Sigma(1660)\frac{1}{2}^+$ . Later, multichannel analyses of the  $\bar{K}N$  reactions

support the existence of the  $\Sigma(1660)\frac{1}{2}^+$  instead of  $\Sigma(1620)\frac{1}{2}^-$  [11]. In Ref. [18], the total cross sections for  $K^-p$  and  $K^-n$  with all proper final states are analyzed and indicate some  $\Sigma$  resonances near 1600 MeV without clear quantum numbers. Reference [19] analyzes the reaction  $K^-n \rightarrow \pi^-\Lambda$  and gets two possible solutions, with one solution indicating a  $\Sigma(\frac{1}{2}^-)$  near 1600 MeV and the other showing no resonant structure below the  $\Sigma(1670)$ . So all claims of evidence for the  $\Sigma(1620)\frac{1}{2}^-$  listed in PDG tables [11] are very shaky. Instead, some reanalyses of the  $\pi\Lambda$  relevant data suggest that there may exist a  $\Sigma(\frac{1}{2}^-)$  resonance around 1380 MeV [20], which supports the prediction of unquenched quark models [5,6].

Some other works [13,21] show support for  $\Sigma(\frac{1}{2}^-)$  with a larger mass, named as the  $\Sigma(1750)\frac{1}{2}^-$  in PDG. Reference [13] analyzes the reaction  $K^-p \rightarrow \pi^0\Lambda$  with the c.m. energy from 1537 to 2215 MeV and gives possible  $\Sigma(\frac{1}{2}^-)$  resonance with mass around 1700 MeV. Reference [21] studies the same reaction with the technique of Barrelet zeros for the partial wave solutions. Seven ambiguous solutions are generated with several of them containing  $\Sigma(\frac{1}{2}^-)$  with mass above 1650 MeV.

To pin down the nature of the lowest  $\frac{1}{2}^-$  SU(3) baryon nonet, it is crucial to find hyperon states of the lowest  $\frac{1}{2}^-$  SU(3) nonet and study their properties systematically. For the study of  $\Sigma$  resonances, the  $\bar{K}N \rightarrow \pi\Lambda$  reaction is the best available channel, where the  $s$ -channel intermediate states are purely hyperons with strangeness  $S = -1$  and isospin  $I = 1$ .

Recently, high-statistic new data for the reaction  $K^-p \rightarrow \pi^0\Lambda$  has been presented by the Crystal Ball collaboration with the c.m. energy of 1560–1676 MeV for both differential cross sections and  $\Lambda$  polarizations [22]. Our previous analysis of the new Crystal Ball data clearly shows that the Crystal Ball  $\Lambda$  polarization data demand the existence of a  $\Sigma$  resonance with  $J^P = \frac{1}{2}^+$  and mass near 1635 MeV [23], compatible with  $\Sigma(1660)\frac{1}{2}^+$  listed in PDG, while the  $\Sigma(1620)\frac{1}{2}^-$  is not needed by the data. The differential cross sections alone cannot distinguish the two solutions with either  $\Sigma(1660)\frac{1}{2}^+$  or  $\Sigma(1620)\frac{1}{2}^-$ .

To further clarify the status of the  $\Sigma(1620)_{\frac{1}{2}}^{-}$  and the  $\Sigma(1635)_{\frac{1}{2}}^{+}$ , here we extend the work of Ref. [23] to analyze the differential cross sections and  $\Lambda$  polarizations for both  $K^- p \rightarrow \pi^0 \Lambda$  and  $K^- n \rightarrow \pi^- \Lambda$  reactions with an effective Lagrangian approach, using the new Crystal Ball data on  $K^- p \rightarrow \pi^0 \Lambda$  with the c.m. energy of 1560–1676 MeV [22], and the  $K^- n \rightarrow \pi^- \Lambda$  data of Ref. [19] with the c.m. energy of 1550–1650 MeV, where the evidence of the  $\Sigma(1620)_{\frac{1}{2}}^{-}$  was claimed.

This paper is organized as follows. In Sec. II, we present the theoretical framework of the analysis. In Sec. III, we present the analysis results and discussions. A brief summary is given in Sec. IV.

## II. THEORETICAL FRAMEWORK

The Feynman diagrams for  $K^- N \rightarrow \pi \Lambda$  are depicted in Fig. 1, where  $k$ ,  $p$ ,  $q$ , and  $p'$  represent the momenta of the incoming  $K^-$ ,  $N$  and the outgoing  $\pi$ ,  $\Lambda$  separately. The main contributions are from the  $t$ -channel  $K^*$  exchange, the  $u$ -channel proton exchange, and the  $s$ -channel  $\Sigma$  and its resonances.

The relevant effective Lagrangians for the hadron couplings are listed in Eqs. (1)–(14):

$$\mathcal{L}_{K^* K \pi} = i g_{K^* K \pi} K_\mu^* (\pi \cdot \tau \partial^\mu K - \partial^\mu \pi \cdot \tau K), \quad (1)$$

$$\mathcal{L}_{K^* N \Lambda} = -g_{K^* N \Lambda} \bar{\Lambda} \left( \gamma_\mu K^{*\mu} - \frac{\kappa_{K^* N \Lambda}}{2M_N} \sigma_{\mu\nu} \partial^\nu K^{*\mu} \right) N, \quad (2)$$

$$\mathcal{L}_{\pi N N} = \frac{g_{\pi N N}}{2M_N} \bar{N} \gamma^\mu \gamma_5 \partial_\mu \pi \cdot \tau N, \quad (3)$$

$$\mathcal{L}_{K N \Lambda} = \frac{g_{K N \Lambda}}{M_N + M_\Lambda} \bar{N} \gamma^\mu \gamma_5 \Lambda \partial_\mu K + \text{H.c.}, \quad (4)$$

$$\mathcal{L}_{K N \Sigma(\frac{1}{2}^+)} = \frac{g_{K N \Sigma}}{M_N + M_\Sigma} \partial_\mu \bar{K} \Sigma \cdot \tau \gamma^\mu \gamma_5 N + \text{H.c.}, \quad (5)$$

$$\mathcal{L}_{\Sigma(\frac{1}{2}^+) \Lambda \pi} = \frac{g_{\Sigma \Lambda \pi}}{M_\Lambda + M_\Sigma} \bar{\Lambda} \gamma^\mu \gamma_5 \partial_\mu \pi \cdot \Sigma + \text{H.c.}, \quad (6)$$

$$\mathcal{L}_{K N \Sigma(\frac{1}{2}^-)} = -i g_{K N \Sigma} \bar{K} \Sigma \cdot \tau N + \text{H.c.}, \quad (7)$$

$$\mathcal{L}_{\Lambda \pi \Sigma(\frac{1}{2}^-)} = -i g_{\Lambda \pi \Sigma} \bar{\Sigma} \Lambda \pi + \text{H.c.}, \quad (8)$$

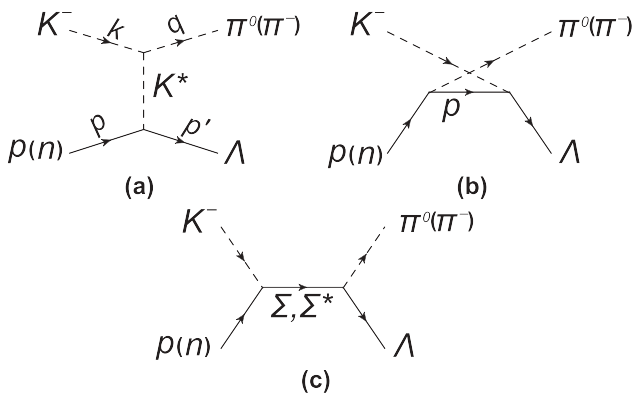


FIG. 1. Feynman diagrams for  $K^- p \rightarrow \pi^0 \Lambda$  and  $K^- n \rightarrow \pi^- \Lambda$ . (a)  $t$ -channel  $K^*$  exchange; (b)  $u$ -channel proton exchange; (c)  $s$ -channel  $\Sigma$  and its resonances exchanges.

$$\mathcal{L}_{K N \Sigma(\frac{3}{2}^+)} = \frac{f_{K N \Sigma}}{m_K} \partial_\mu \bar{K} \Sigma^\mu \cdot \tau N + \text{H.c.}, \quad (9)$$

$$\mathcal{L}_{\Sigma(\frac{3}{2}^+) \Lambda \pi} = \frac{f_{\Sigma \Lambda \pi}}{m_\pi} \partial_\mu \bar{\pi} \cdot \bar{\Sigma}^\mu \Lambda + \text{H.c.}, \quad (10)$$

$$\mathcal{L}_{K N \Sigma(\frac{3}{2}^-)} = \frac{f_{K N \Sigma}}{m_K} \partial_\mu \bar{K} \Sigma^\mu \cdot \tau \gamma_5 N + \text{H.c.}, \quad (11)$$

$$\mathcal{L}_{\Sigma(\frac{3}{2}^-) \Lambda \pi} = \frac{f_{\Sigma \Lambda \pi}}{m_\pi} \partial_\mu \bar{\pi} \Sigma^\mu \gamma_5 \Lambda + \text{H.c.}, \quad (12)$$

$$\mathcal{L}_{K N \Sigma(\frac{5}{2}^-)} = g_{K N \Sigma} \partial_\mu \partial_\nu \bar{K} \Sigma^{\mu\nu} \cdot \tau N + \text{H.c.}, \quad (13)$$

$$\mathcal{L}_{\Sigma(\frac{5}{2}^-) \Lambda \pi} = g_{\Lambda \pi \Sigma} \partial_\mu \partial_\nu \bar{\pi} \cdot \bar{\Sigma}^{\mu\nu} \Lambda + \text{H.c.} \quad (14)$$

The value ranges of the coupling constants or parameters are used exactly the same as those in Ref. [23]. Interested readers may refer to Ref. [23] for the detailed descriptions of our effective Lagrangians.

Note that the isospin structures are contained in the Lagrangians; for example, the  $K^* K \pi$  coupling is  $\bar{K}^* \pi \cdot \tau K$ , with

$$\bar{K}^* = (K^{*-}, \bar{K}^{*0}), \quad \pi \cdot \tau = \begin{pmatrix} \pi^0 & \sqrt{2}\pi^+ \\ \sqrt{2}\pi^- & -\pi^0 \end{pmatrix},$$

$$K = \begin{pmatrix} K^+ \\ K^0 \end{pmatrix};$$

and for the  $K N \Sigma$  coupling the isospin structure is  $\bar{K} \Sigma \cdot \tau N$ , with

$$\bar{K} = (K^-, \bar{K}^0), \quad \bar{\Sigma} \cdot \tau = \begin{pmatrix} \bar{\Sigma}^0 & \sqrt{2}\bar{\Sigma}^+ \\ \sqrt{2}\bar{\Sigma}^- & -\bar{\Sigma}^0 \end{pmatrix},$$

$$N = \begin{pmatrix} p \\ n \end{pmatrix}.$$

For each vertex of these channels, the following form factor is used to describe the off-shell properties of the amplitudes:

$$F_B(q_{\text{ex}}^2, M_{\text{ex}}) = \frac{\Lambda^4}{\Lambda^4 + (q_{\text{ex}}^2 - M_{\text{ex}}^2)^2}, \quad (15)$$

where  $q_{\text{ex}}$  and  $M_{\text{ex}}$  denote the four-momenta and mass of the exchanged hadron, respectively. The cutoff parameter  $\Lambda$  is constrained between 0.8 and 1.5 GeV for all channels.

For the propagators with four-momenta  $p$ , we use

$$\frac{-g_{\mu\nu} + p^\mu p^\nu / m_{K^*}^2}{p^2 - m_{K^*}^2} \quad (16)$$

for  $K^*$  meson exchange ( $\mu$  and  $\nu$  are polarization index of  $K^*$ ),

$$\frac{\not{p} + m}{p^2 - m^2} \quad (17)$$

for spin- $\frac{1}{2}$  propagator,

$$\frac{\not{p} + m}{p^2 - m^2} \left( -g^{\mu\nu} + \frac{\gamma^\mu \gamma^\nu}{3} + \frac{\gamma^\mu p^\nu - \gamma^\nu p^\mu}{3m} + \frac{2p^\mu p^\nu}{3m^2} \right) \quad (18)$$

for spin- $\frac{3}{2}$  propagator, and

$$\frac{\not{p} + m}{p^2 - m^2} S_{\alpha\beta\mu\nu}(p, m) \quad (19)$$

for spin- $\frac{5}{2}$  propagator, with

$$S_{\alpha\beta\mu\nu}(p, m) = \frac{1}{2}(\tilde{g}_{\alpha\mu}\tilde{g}_{\beta\nu} + \tilde{g}_{\alpha\nu}\tilde{g}_{\beta\mu}) - \frac{1}{5}\tilde{g}_{\alpha\beta}\tilde{g}_{\mu\nu} - \frac{1}{10}(\tilde{\gamma}_\alpha\tilde{\gamma}_\mu\tilde{g}_{\beta\nu} + \tilde{\gamma}_\alpha\tilde{\gamma}_\nu\tilde{g}_{\beta\mu} + \tilde{\gamma}_\beta\tilde{\gamma}_\mu\tilde{g}_{\alpha\nu} + \tilde{\gamma}_\beta\tilde{\gamma}_\nu\tilde{g}_{\alpha\mu}), \quad (20)$$

$$\tilde{g}_{\mu\nu} = g_{\mu\nu} - \frac{p_\mu p_\nu}{m^2}, \quad \tilde{\gamma}_\mu = \gamma_\mu - \frac{p_\mu}{m^2} \not{p}. \quad (21)$$

For unstable resonances, we replace the denominator  $\frac{1}{p^2 - m^2}$  in the propagators by the Breit-Wigner form  $\frac{1}{p^2 - m^2 + im\Gamma}$ , and replace  $m$  in the rest of the propagators by  $\sqrt{p^2}$ . The  $m$  and  $\Gamma$  in the propagators represent the mass and total width of a resonance, respectively. Because all hyperon states we include have rather narrow width with  $\Gamma \ll m$ , the pole positions for the states are basically  $m - i\Gamma/2$ .

The differential cross sections for  $K^- N \rightarrow \pi \Lambda$  can be expressed as

$$\frac{d\sigma_{\pi\Lambda}}{d\Omega} = \frac{d\sigma_{\pi\Lambda}}{2\pi d\cos\theta} = \frac{1}{64\pi^2 s} \frac{|\mathbf{q}|}{|\mathbf{k}|} |\overline{\mathcal{M}}|^2, \quad (22)$$

where  $\theta$  is the angle between the outgoing  $\pi$  and the beam direction in the c.m. frame;  $s = (p + k)^2$ , and  $\mathbf{k}$  and  $\mathbf{q}$  denote the three-momenta of  $K^-$  and  $\pi$  in the c.m. frame, respectively.  $|\overline{\mathcal{M}}|^2$  denotes the spin-averaged amplitude squared of the reaction.

The  $\Lambda$  polarization in  $K^- N \rightarrow \pi \Lambda \rightarrow \pi\pi N$  can be expressed as

$$P_\Lambda = \frac{3}{\alpha_\Lambda} \left( \int \cos\theta' \frac{d\sigma_{K^- N \rightarrow \pi \Lambda \rightarrow \pi\pi N}}{d\Omega d\Omega'} d\Omega' \right) / \frac{d\sigma_{\pi\Lambda}}{d\Omega}, \quad (23)$$

where  $\alpha_\Lambda = 0.65$ , and  $d\Omega' = d\cos\theta' d\phi'$  is the sphere space of the outgoing nucleon in the  $\Lambda$  rest frame, and  $\theta'$  is the angle between the outgoing nucleon and the vector  $\mathbf{v} = \mathbf{k} \times \mathbf{q}$ , which is perpendicular to the  $K^- N \rightarrow \pi \Lambda$  reaction plane.

For  $\Lambda \rightarrow \pi N$ , the effective Lagrangian is

$$\mathcal{L}_{\Lambda\pi N} = G_F m_\pi^2 \overline{N}(A - B\gamma_5)\Lambda, \quad (24)$$

where  $G_F$  is the Fermi coupling constant;  $A$  and  $B$  are effective coupling constants.

The differential cross section for  $K^- N \rightarrow \pi \Lambda \rightarrow \pi\pi N$  can be expressed as

$$\frac{d\sigma_{K^- N \rightarrow \pi \Lambda \rightarrow \pi\pi N}}{d\Omega d\Omega'} = \frac{|\mathbf{q}||\mathbf{p}'_N| |\overline{\mathcal{M}}|^2}{32^2 2\pi m_\Lambda^2 \Gamma_\Lambda s |\mathbf{k}|}, \quad (25)$$

where  $\mathbf{p}'_N$  denotes the three-momenta of the produced nucleon in the  $\Lambda$  rest frame, and  $\Gamma_\Lambda$  is  $\Lambda$  decay width.  $\overline{\mathcal{M}}$  denotes the amplitude of the reaction  $K^- N \rightarrow \pi \Lambda \rightarrow \pi\pi N$ , and  $|\overline{\mathcal{M}}|^2 = \frac{1}{2} \sum_{s_1, s_3} \mathcal{M}' \mathcal{M}'^\dagger$  is the spin-averaged amplitude squared.

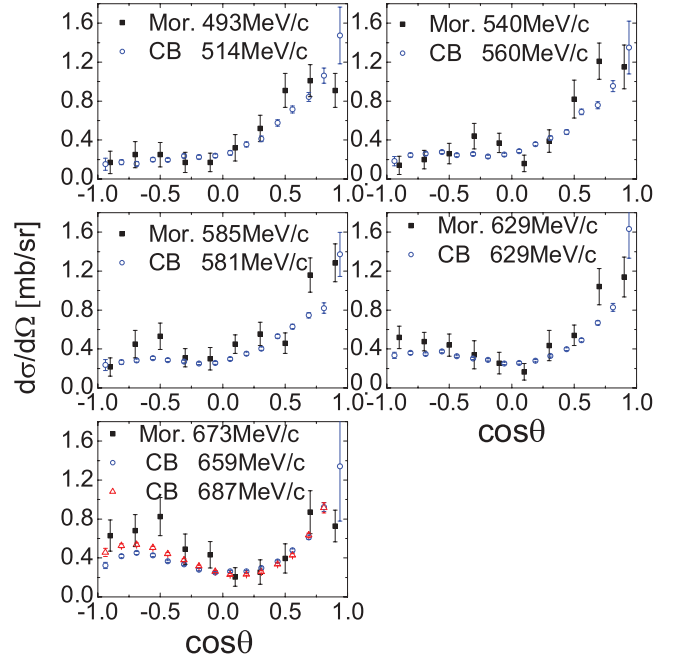


FIG. 2. (Color online) Comparison of the differential cross sections of Ref. [19] with that of the Crystal Ball [22] of similar beam momenta, scaled with consideration of isospin relations.

### III. RESULTS AND DISCUSSIONS

The isospin structures of the couplings require the cross section of  $K^- p \rightarrow \pi^0 \Lambda$  to be half that of the  $K^- n \rightarrow \pi^- \Lambda$ . In Fig. 2, we compare twice of the Crystal Ball data [22] of the differential cross sections with that of Ref. [19] in similar beam momenta. One can see that, in general, the data of the two experiments are compatible with each other within statistic uncertainties.

In our analysis, the  $t$ -channel  $K^*$  exchange and the  $u$ -channel proton exchange amplitudes are fundamental ingredients. The well-established four-star  $\Sigma(1189)_{\frac{1}{2}}^{1+}$ ,  $\Sigma(1385)_{\frac{3}{2}}^{3+}$ ,  $\Sigma(1670)_{\frac{3}{2}}^{3-}$ , and  $\Sigma(1775)_{\frac{5}{2}}^{5-}$  contributions are always included in the analysis. The ranges of the parameters have been constrained from the relevant PDG values or model predictions, which have been explained in Sec. II of Ref. [23]. The mass of  $\Sigma(1775)_{\frac{5}{2}}^{5-}$  is much larger than the energy range of the experiments, and the analysis is expected to be insensitive to the parameters of  $\Sigma(1775)$  resonance. Thus we fix the mass, width, and coupling constant of the  $\Sigma(1775)$  to be the PDG central values. The fixed parameters of  $\Sigma(1189)_{\frac{1}{2}}^{1+}$ ,

TABLE I. Fixed parameters for  $\Sigma(1189)_{\frac{1}{2}}^{1+}$ ,  $\Sigma(1385)_{\frac{3}{2}}^{3+}$ , and  $\Sigma(1775)_{\frac{5}{2}}^{5-}$ .

	Mass (MeV)	$\Gamma$ (MeV)	$\sqrt{\Gamma_{\pi\Lambda}\Gamma_{\overline{K}N}}/\Gamma_{\text{tot}}$
$\Sigma(1189)_{\frac{1}{2}}^{1+}$	1192.6	0	
$\Sigma(1385)_{\frac{3}{2}}^{3+}$	1384	36	
$\Sigma(1775)_{\frac{5}{2}}^{5-}$	1775	120	0.28

TABLE II. Adjusted parameters for  $\Sigma(1670)\frac{3}{2}^-$  and  $\Sigma(1660)\frac{1}{2}^+$  resonances.

	Mass (MeV) (PDG estimate)	$\Gamma_{\text{tot}}$ (MeV) (PDG estimate)	$\sqrt{\Gamma_{\pi\Lambda}\Gamma_{\bar{K}N}}/\Gamma_{\text{tot}}$ (PDG range)
$\Sigma(1670)\frac{3}{2}^-$	$1673 \pm 1(1665, 1685)$	$52_{-2}^{+5}(40, 80)$	$0.081_{-0.004}^{+0.002}(0.018, 0.17)$
$\Sigma(1660)\frac{1}{2}^+$	$1633 \pm 3(1630, 1690)$	$121_{-7}^{+4}(40, 200)$	$-0.064_{-0.003}^{+0.005}(-0.065, 0.24)$

$\Sigma(1385)\frac{3}{2}^+$ , and  $\Sigma(1775)\frac{5}{2}^-$  are shown in Table I (other tunable parameters are shown in Table II and III).

From analysis of the differential cross sections as well as the  $\Lambda$  polarizations of the two experiments with the above six channels and 14 tunable parameters constrained in the appropriate ranges, we obtain a fit with  $\chi^2$  of 1680 for the total 348 data points. Here we only include the statistical errors presented by the Crystal Ball (CB) experiment. For the CB differential cross section data, there is an overall systematical uncertainty of about 7%. Because the systematical uncertainty for the CB data is mainly for the normalization, the  $\Lambda$  polarization defined by Eq. (23) does not suffer such systematical uncertainty. Later we show that for disentangling the ambiguity of spin-parity of  $1/2^+$  or  $1/2^-$  for an additional  $\Sigma$  resonance it is mainly determined by  $\Lambda$  polarization data and hence does not suffer from such systematical uncertainty.

To get an acceptable good fit of the experimental data, we need to introduce some other  $\Sigma$  resonances in the  $s$  channel, with its coupling constant, mass, and width as free parameters. Among the  $J^P = \frac{1}{2}^\pm, \frac{3}{2}^\pm$   $\Sigma$  resonances, we find that the best fit is given by including a  $J^P = \frac{1}{2}^+$  resonance with mass near 1633 MeV, width around 120 MeV, and couplings  $\sqrt{\Gamma_{\pi\Lambda}\Gamma_{\bar{K}N}}/\Gamma_{\text{tot}} \sim -0.064$ , where the negative sign means that the couplings to  $\pi\Lambda$  and  $\bar{K}N$  have opposite signs. The analysis includes 18 tunable parameters in the allowed range and the  $\chi^2$  for this best fit is 572 for the total 348 data points. The improvement is huge with  $\Delta\chi^2 = 1008$  for 348 data points.

Figures 3 and 4 show our analysis results for the differential cross sections and the  $\Lambda$  polarizations of the reaction compared with the experimental data from Refs. [19,22], respectively. We can see that the results are generally in good agreement with the data, and the fit (especially, the  $\Lambda$  polarization in Fig. 4) is much improved by including the  $\Sigma(1633)\frac{1}{2}^+$ . In Fig. 3 we also show the second solution of Ref. [19], which suggests a  $\Sigma(\frac{1}{2}^-)$  resonance with mass at 1600 MeV and width around 87 MeV. The solution of Ref. [19] fits the old data well; however, one can see that the large error bars of the old data can accommodate very different solutions, and the high-precision new data of CB can distinguish different solutions more efficiently.

If we introduce the new resonance of other  $J^P$  quantum numbers instead of introducing the  $\Sigma(1633)\frac{1}{2}^+$  resonance, the  $\chi^2$  value is worse by 327 for  $J^P = \frac{1}{2}^-$ , 371 for  $J^P = \frac{3}{2}^+$ , and 820 for  $J^P = \frac{3}{2}^-$ , respectively. Our analysis with data of the two groups clearly supports the existence of  $\Sigma(\frac{1}{2}^+)$  resonance near 1633 MeV. Further analysis with data from more groups and wider energy ranges in the future will be helpful to verify our results.

In Table II, we give the central values and uncertainties for the six parameters of  $\Sigma(1670)\frac{3}{2}^-$  and  $\Sigma(1633)\frac{1}{2}^+$  resonances. We can see that the mass and width of the  $\Sigma(1670)$  in our fit are compatible with the PDG estimates [11]. The characters of  $\Sigma(\frac{1}{2}^+)$  from our analysis are consistent with the three-star  $\Sigma(1660)\frac{1}{2}^+$  in PDG, with more precise values for the mass, width, and couplings.

The other 12 tunable parameters in our study include five coupling constants and seven cutoff parameters. In Table III, we show the fitted results of the five coupling constants of the  $t$ -channel,  $u$ -channel, and  $s$ -channel  $\Sigma(1189)$  and  $\Sigma(1385)\frac{3}{2}^+$  exchanges.

All the fitted parameters listed in Tables II and III are consistent with those given in Ref. [23] within error bars. The error bars listed here are smaller than those of Ref. [23]. The main reason is that we made a careless mistake in Ref. [23]: The output of the  $\chi^2/2$  value was mistaken as the  $\chi^2$  value. The values of all the  $\chi^2$  in Ref. [23] should be doubled. Another reason is that here we include data of the  $K^-n \rightarrow \pi^- \Lambda$  reaction in addition.

For the fit with  $\Sigma(\frac{1}{2}^-)$ , instead of including the  $\Sigma(1633)\frac{1}{2}^+$ , the fitted mass goes down to our preset lower limit 1360 MeV, with width and coupling constant  $g_{KN\Sigma}g_{\Sigma\pi\Lambda}$  to be 312 MeV and  $-1.253$ , respectively. So even in the case without including the  $\Sigma(1633)\frac{1}{2}^+$ , the data prefer a low mass  $\Sigma(\frac{1}{2}^-)$ , as indicated in Refs. [7,20], rather than the  $\Sigma(1620)\frac{1}{2}^-$ , as listed in PDG [11].

When including both  $\Sigma(1633)\frac{1}{2}^+$  and an additional  $\Sigma(\frac{1}{2}^-)$  in the  $s$  channel, we get a lowest  $\chi^2$  of 548 for the total 348 data points with 22 tunable parameters. The fitted mass and width of  $\Sigma(\frac{1}{2}^-)$  are 1432 and  $\geq 1000$  MeV, respectively.

From the above results, the  $\Sigma(1620)\frac{1}{2}^-$  is not supported from our analysis at all. This seems differing from the

TABLE III. Adjusted coupling constants for  $t$ -channel,  $u$ -channel, and  $s$ -channel  $\Sigma(1189)$  and  $\Sigma(1385)\frac{3}{2}^+$  exchanges.

$g_{K^*N\Lambda}$ (Model range)	$g_{K^*N\Lambda}K^*N\Lambda$ (Model range)	$g_{\pi NN}g_{KN\Lambda}$ [SU(3)]	$g_{KN\Sigma}g_{\Sigma\Lambda\pi}$ [SU(3)]	$f_{KN\Sigma^*}f_{\Sigma^*\Lambda\pi}$ [SU(3)]
$-6.10_{-0}^{+0.07}(-6.11, -4.26)$ [24]	$-11.33_{-0.06}^{+0}(-16.3, -10.4)$ [24]	$-178_{-7}^{+2}(-176)$	$49.2_{-0.9}^{+0}(34.8)$	$-3.94_{-0.13}^{+0.32}(-4.1)$



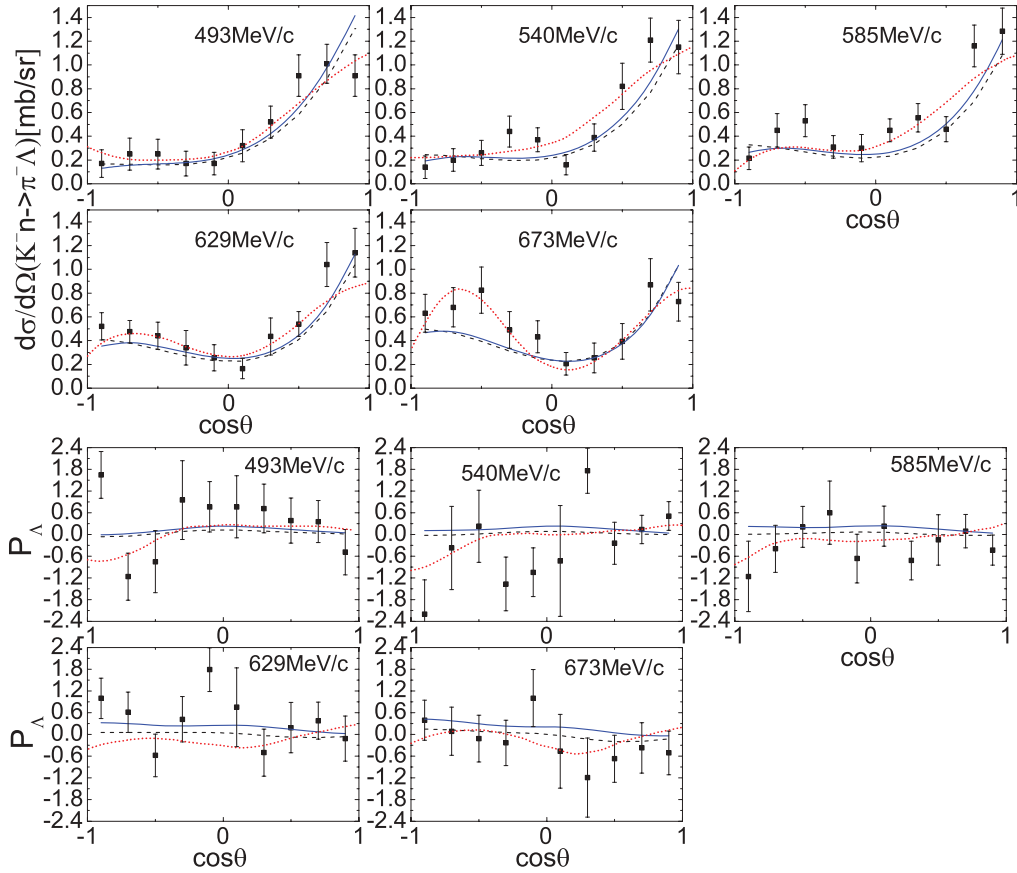


FIG. 3. (Color online) The differential cross sections and  $\Lambda$  polarizations of the reaction  $K^- n \rightarrow \pi^- \Lambda$ , compared with the experimental data of Ref. [19] and its original second solution including a  $\Sigma(\frac{1}{2}^-)$  resonance with mass about 1600 MeV (red dotted lines), with incident  $K^-$  momenta from 493 to 673 MeV/c in the laboratory frame and  $\theta$  the angle between outgoing  $\pi^-$  and incoming  $K^-$  in the c.m. frame. The dashed and solid (blue) lines are the best fits by including only the four well established  $\Sigma$  resonances in the  $s$  channel and by including an additional  $\Sigma(\frac{1}{2}^+)$  with mass around 1633 MeV, respectively.

results of Ref. [19], where one of its solutions supports the  $\Sigma(1620)\frac{1}{2}^-$ , although another one of its solutions does not need it. The major difference of two analyses is the treatment of nonresonant background contribution. In Ref. [19], “a particular partial wave was assumed to be either resonant or background but not both” and background contributions in each partial wave are independent, while in our approach the background contributions in each partial waves are determined by the  $t$ -channel  $K^*$  exchange and  $u$ -channel proton exchange. If we only fit the data of Ref. [19] with the effective Lagrangian approach, with just the four established  $\Sigma$  resonances in the  $s$  channel, together with the  $t$ -channel and  $u$ -channel contributions, we obtain a  $\chi^2$  of 116 for the total 100 data points, which is already much smaller than the  $\chi^2$  value of 176–180 for both solutions of Ref. [19]. We think our approach is more physical and appropriate in describing the reactions. Including the  $\Sigma(1633)\frac{1}{2}^+$  in addition will further reduce the  $\chi^2$  to 109. The old  $K^- n \rightarrow \pi^- \Lambda$  data with large error bars show marginal evidence for the  $\Sigma(1633)\frac{1}{2}^+$ . It is mainly the new precise CB data on  $\Lambda$  polarizations demanding the existence of the  $\Sigma(1633)\frac{1}{2}^+$ .

Taking the four four-star  $\Sigma$  resonances and the three-star  $\Sigma(\frac{1}{2}^+)$  with tunable parameters as basic contributions, we further examine whether any other additional resonance can make significant improvement to the fit.

The largest improvement is given by including an additional  $\Sigma(\frac{3}{2}^+)$  resonance with a mass of 1840 MeV or above. The  $\chi^2$  reaches 487 for the total 348 data points, with the resonance having a coupling  $\sqrt{\Gamma_{\pi\Lambda}\Gamma_{\bar{K}N}}/\Gamma_{\text{tot}} \sim 0.289$  and width around 271 MeV. Note there are two  $\Sigma(\frac{3}{2}^+)$  resonances above 1800 MeV listed in PDG [11], that is, one-star  $\Sigma(1840)$  and two-star  $\Sigma(2080)$ . With this solution, the mass and width of the  $\Sigma(\frac{1}{2}^+)$  shift to 1632 and 93 MeV, respectively.

When including a  $\Sigma(\frac{3}{2}^-)$  resonance, the best  $\chi^2$  is 535 for the total 348 data points, with resulting mass around 1542 MeV, width about 25.6 MeV, and couplings  $\sqrt{\Gamma_{\pi\Lambda}\Gamma_{\bar{K}N}}/\Gamma_{\text{tot}} \sim 0.0374$ . This solution improves the  $\chi^2$  by 37 and seems consistent with the resonance structure  $\Sigma(1560)$  or  $\Sigma(1580)\frac{3}{2}^-$  in PDG. Reference [25] also proposes a  $\Sigma(\frac{3}{2}^-)$  resonance with mass around 1570 MeV and width about 60 MeV from the  $\bar{K}N\pi$  system. The inclusion of  $\Sigma(\frac{3}{2}^-)$  in the

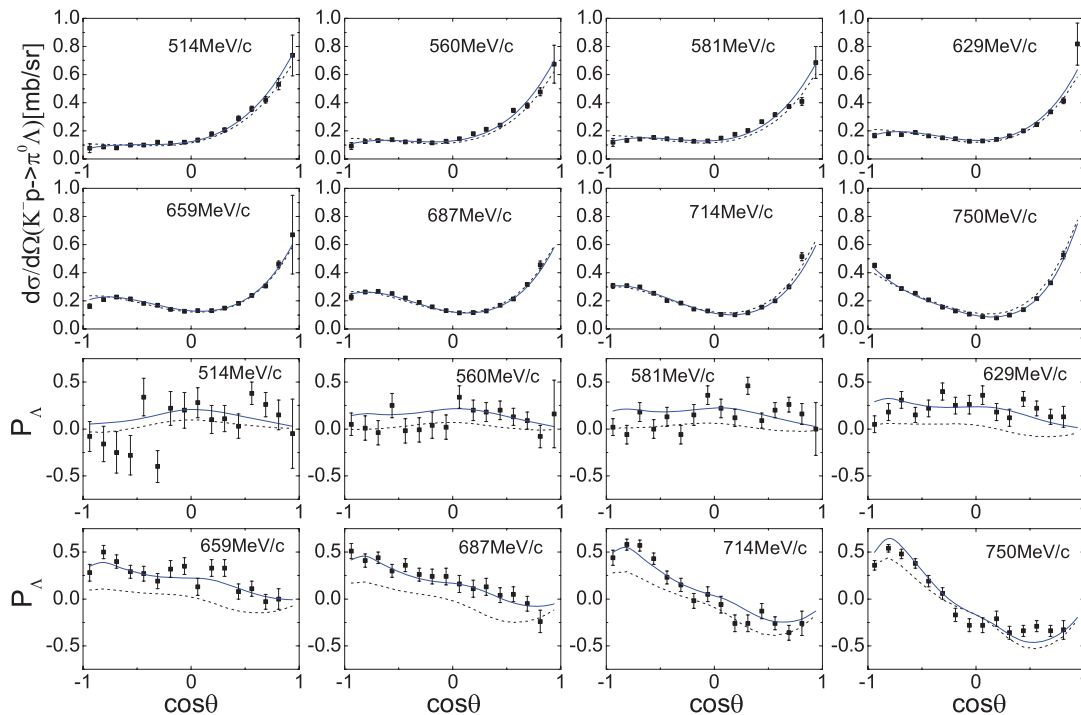


FIG. 4. (Color online) The differential cross sections and  $\Lambda$  polarizations for the reaction  $K^- p \rightarrow \pi^0 \Lambda$ , compared with the new CB data [22], where  $\theta$  is the angle between outgoing  $\pi^0$  and incoming  $K^-$  in the c.m. frame. The dashed and solid (blue) lines are the best fits by including only four established  $\Sigma$  resonances in the  $s$  channel and by including an additional  $\Sigma(1633)_{\frac{1}{2}}^{1+}$  in the  $s$  channel, respectively.

analysis makes the mass and width of the  $\Sigma(\frac{1}{2}^+)$  shift to 1634 and 130 MeV, respectively.

When including an additional  $\Sigma(\frac{1}{2}^+)$  resonance, we get a  $\chi^2$  of 541 with mass 1610 MeV, width 20 MeV, and  $\sqrt{\Gamma_{\pi\Lambda}\Gamma_{\bar{K}N}}/\Gamma_{\text{tot}} \sim -0.032$  for the additional  $\Sigma(\frac{1}{2}^+)$ . This resonance seems consistent with the  $\Sigma(1620)$  resonance with unknown quantum numbers listed in PDG [11]. With the additional  $\Sigma(\frac{1}{2}^+)$  in analysis, the mass, width, and  $\sqrt{\Gamma_{\pi\Lambda}\Gamma_{\bar{K}N}}/\Gamma_{\text{tot}}$  of the  $\Sigma(1633)_{\frac{1}{2}}^{1+}$  shift to 1647 MeV, 91 MeV, and  $-0.065$ . This solution appears to support the results of Ref. [26], where both  $\Sigma(1620)_{\frac{1}{2}}^{1+}$  and  $\Sigma(1660)_{\frac{1}{2}}^{1+}$  are predicted. Although the  $\chi^2$  is only improved by 31 with the inclusion of two  $\Sigma(\frac{1}{2}^+)$  resonances at 1610 and 1647 MeV, compared with the case of the single  $\Sigma(1633)_{\frac{1}{2}}^{1+}$ , the existence of such two resonances cannot be excluded. The contribution of the  $\Sigma(1633)_{\frac{1}{2}}^{1+}$  seems to have similar effects with the two  $\Sigma(\frac{1}{2}^+)$  around with narrower widths.

Some uncertainty may still exist from the uncertainties in some coupling constants and cutoffs; however, the main results of this analysis will not change.

#### IV. SUMMARY

To further clarify the properties of the  $\Sigma$  resonances, we analyze the differential cross sections and  $\Lambda$  polarizations for the reactions  $K^- n \rightarrow \pi^- \Lambda$  and  $K^- p \rightarrow \pi^0 \Lambda$  with the effective Lagrangian method. The experimental data are adopted from the new high-statistic CB experiment [22] and an early report of Ref. [19], with the c.m. energy 1550–1676 MeV.

In our calculation, the contributions of the  $ft$ -channel  $K^*$  exchange,  $u$ -channel proton exchange, and the four-star  $\Sigma$  resonances exchanges in the  $s$  channel, that is,  $\Sigma(1189)$ ,  $\Sigma(1385)$ ,  $\Sigma(1670)$ , and  $\Sigma(1775)$ , are always included. These ingredients are still insufficient to describe the experimental data, with  $\chi^2$  about 1680 for the total 348 data points. An additional  $\Sigma(\frac{1}{2}^+)$  with mass around 1633 MeV and width about 120 MeV is absolutely necessary to reach an acceptable good fit. It reduces the  $\chi^2$  to 572 for the total 348 data points. Its properties are consistent with the  $\Sigma(1660)_{\frac{1}{2}}^{1+}$  listed in PDG.

In searching for the lightest  $\Sigma(\frac{1}{2}^-)$ , our results do not show any evidence for the  $\Sigma(1620)_{\frac{1}{2}}^{1-}$  resonance listed as a two-star resonance in PDG; a  $\Sigma(\frac{1}{2}^-)$  with much lower mass, as suggested by the pentaquark models [5,6], cannot be excluded. The indications of the other additional  $\Sigma$  resonance structures are also discussed, with possible  $\Sigma(\frac{3}{2}^-)$  resonance of mass around 1542 MeV,  $\Sigma(\frac{3}{2}^+)$  with mass around 1840 MeV or above, and additional  $\Sigma(\frac{1}{2}^+)$  near 1610 MeV.

#### ACKNOWLEDGMENTS

Helpful discussions with Jia-Jun Wu and Xu Cao are gratefully acknowledged. This work is supported in part by the National Natural Science Foundation of China under Grants No. 10905059, No. 11035006, and No. 11261130311 (CRC110 by DFG and NSFC), the Chinese Academy of Sciences under Project No. KJCX2-EW-N01, and the Ministry of Science and Technology of China (2009CB825200).

- [1] S. Capstick and W. Roberts, *Prog. Part. Nucl. Phys.* **45**, S241 (2000).
- [2] S. Capstick and N. Isgur, *Phys. Rev. D* **34**, 2809 (1986).
- [3] L. Y. Glozman and D. O. Riska, *Phys. Rep.* **268**, 263 (1996).
- [4] U. Loring, B. C. Metsch, and H. R. Petry, *Eur. Phys. J. A* **10**, 395 (2001).
- [5] C. Helminen and D. O. Riska, *Nucl. Phys. A* **699**, 624 (2002).
- [6] A. Zhang *et al.*, *High Energy Phys. Nucl. Phys.* **29**, 250 (2005).
- [7] B. S. Zou, *Nucl. Phys. A* **835**, 199 (2010); *Eur. Phys. J. A* **35**, 325 (2008).
- [8] Y. Oh, *Phys. Rev. D* **75**, 074002 (2007).
- [9] K. P. Khemchandani, A. Martinez Torres, H. Kaneko, H. Nagahiro, and A. Hosaka, *Phys. Rev. D* **84**, 094018 (2011).
- [10] A. Ramos, E. Oset, and C. Bennhold, *Phys. Rev. Lett.* **89**, 252001 (2002).
- [11] J. Beringer *et al.* (Particle Data Group), *Phys. Rev. D* **86**, 010001 (2012).
- [12] P. Baillon and P. J. Litchfield, *Nucl. Phys. B* **94**, 39 (1975).
- [13] A. J. Van Horn, *Nucl. Phys. B* **87**, 157 (1975).
- [14] A. de Bellefon and A. Berthon, *Nucl. Phys. B* **109**, 129 (1976).
- [15] R. A. Ponte *et al.*, *Phys. Rev. D* **12**, 2597 (1975).
- [16] J. K. Kim, *Phys. Rev. Lett.* **27**, 356 (1971).
- [17] W. Langbein and F. Wagner, *Nucl. Phys. B* **47**, 477 (1972).
- [18] A. S. Carroll *et al.*, *Phys. Rev. Lett.* **37**, 806 (1976).
- [19] W. A. Morris, J. R. Albright, A. P. Colleraine, J. D. Kimel, and J. E. Lannutti, *Phys. Rev. D* **17**, 55 (1978).
- [20] J. J. Wu, S. Dulat, and B. S. Zou, *Phys. Rev. D* **80**, 017503 (2009); *Phys. Rev. C* **81**, 045210 (2010); P. Gao, J. J. Wu, and B. S. Zou, *ibid.* **81**, 055203 (2010).
- [21] A. J. Van Horn, *Nucl. Phys. B* **87**, 145 (1975).
- [22] S. Prakhov *et al.*, *Phys. Rev. C* **80**, 025204 (2009).
- [23] Puze Gao, B. S. Zou, and A. Sibirtsev, *Nucl. Phys. A* **867**, 41 (2011).
- [24] V. G. J. Stoks and Th.A. Rijken, *Phys. Rev. C* **59**, 3009 (1999); Y. Oh and H. Kim, *ibid.* **73**, 065202 (2006).
- [25] A. Gal and H. Garcilazo, *Nucl. Phys. A* **864**, 153 (2011).
- [26] A. Martinez Torres, K. P. Khemchandani, and E. Oset, *Phys. Rev. C* **77**, 042203 (2008).